ISSN 2179-3956

CHARACTERIZATION OF THE CRITICAL LOAD/SPEED VALUES TO MILD TO SEVERE WEAR REGIME TRANSITION IN A PIN-ON-DISC TEST OF A DENSE ALUMINA[1]

Nadetsa Reginato Tedesco[2]
Elíria Maria de Jesus Agnolon Pallone[3]
Roberto Tomasi[4]

Abstract
Alumina ceramics in a wear test reacts with air humidity to form a film layer of aluminum hydroxide which acts as a lubricant. Increasing sliding test load and/or speed affects the tribofilm and changes the wear regime from mild to severe. The purpose of this work was to determine critical values of load and sliding speed for the wear regime transition under controlled atmosphere humidity, in a pin-on-disc test. The wear rate and the worn surface SEM image and roughness allowed to distinguish the mild and severe wear regime for different speed/load combinations so that the boundaries of mild wear region was determined. The boundaries were characterized by a narrow transition zone. The image analyses have shown distinct wear mechanisms as function of sliding speed and load.
Key words: Wear resistance; Alumina; Ceramic; Pin-on-disc.

CARACTERIZAÇÃO DOS VALORES DE CARGA/VELOCIDADE CRÍTICOS PARA A TRANSIÇÃO DO DESGASTE BRANDO PARA SEVERO EM ENSAIO PINO NO DISCO DE ALUMINA DENSA

Resumo
Sob ação de desgaste a alumina reage com a umidade do ar formando uma película de hidróxido de alumínio que atua como lubrificante. O aumento da carga e/ou da velocidade de deslizamento afeta o comportamento do tribofilme e muda o tipo de desgaste, de brando para severo. O objetivo deste trabalho foi determinar os valores críticos de carga e velocidade de deslizamento para a transição do tipo de desgaste, sob umidade do ar controlada, em ensaio do tipo pino no disco. A taxa de desgaste e a rugosidade e imagem de MEV das superfícies desgastadas permitiram distinguir o tipo de desgaste para diferentes combinações de carga e velocidade, de modo a determinar os limites da região de desgaste brando. O limite observado se caracterizou por uma zona de transição estreita. A análise de imagens mostrou a ocorrência de diferentes mecanismos de desgaste em função da velocidade e da carga empregadas.
Palavras-chave: Desgaste; Alumina; Materiais Cerâmicos; Pino no disco.

[1] *Technical contribution to the First International Brazilian Conference on Tribology – TriboBr-2010, November, 24th-26th, 2010, Rio de Janeiro, RJ, Brazil.*
[2] *Graduate Student, Post-graduate Program in Materials Science and Engineering, Federal University of São Carlos, São Carlos – SP – Brazil.*
[3] *PhD, Basics Science Department-FZEA, University of São Paulo, Pirassununga – SP – Brazil.*
[4] *PhD, Materials Engineering Department, Federal University of São Carlos, São Carlos – SP – Brazil.*

ISSN 2179-3956

1 INTRODUCTION

Numerous studies have been conducted on the sliding wear behaviors of advanced ceramic such as Si_3N_4, SiC, Al_2O_3 and ZrO_2. Among the different types of engineering ceramics, alumina is the most widely used material due to favorable properties in a wide range of applications and to a relatively good cost-effectiveness. [1] The distinguish wear and friction properties of this dense ceramic most of the time are related to the aluminium hydroxide tribofilm formation, which can consist of fine wear particles, or so called debris, smashed and embed in the surface voids. Due to repeated movement, these particles react with the water vapor in the environment making the surface smoother decreasing wear and friction.[2-6] Several researches have addressed the characterization of the tribofilms and the debris and their role on the wear behavior.[6-9]

Also, published literature shows a large variability in the wear of alumina ceramics due to the test variables (applied load,[10,11] environment,[2-9,12] sliding speed [1,11,13] and distance,[11,14] temperature[8,10,15] and test configuration[16]) since wear resistance is not an intrinsic property but rather a response which is governed by these test conditions. Alumina wear rates have been reported to be in a wide range of magnitudes, from 10^{-3} $mm^3/N.m$ to 10^{-9} $mm^3/N.m$[13] and it is a common sense to separate the wear behavior in two wear regime: mild and severe.[1,15,17-19] These two conditions of wear regime are well defined and a narrow transition from the 'mild' condition to 'severe' have been reported as a result of the alteration of operating parameters. The limit between the two conditions has been empirically observed by distinguishing the wear regime by the wear rate and worn surface characteristics such as roughness, grooves, delamination, cracks and wear mechanism. Mild regime presents a smooth surface and wear rates below 10^{-6} $mm^3/N.m$ while 'severe' presents a rough surface (most of the time higher than the grain size), wear rates under 10^{-6} or 10^{-5} $mm^3/N.m$ and presents intergranular fracture at the worn surface.[17-19]

Considering the above mentioned variability in the measured wear resistance of alumina and since tribochemical reactions can have a beneficial effect when the resultant reaction product is stable, reducing friction and wear, the study and characterization of the test parameters which allow the formation and stability of the tribofilm is necessary to allow future controlled pin-on-disc tests of different alumina materials. Taking this in account, the aim of this work was to set up the combinations of sliding speed and applied load and recognize then within the severe or mild wear regime in a full dense alumina in an unlubricated pin-on-disc wear test.

2 MATERIALS AND METHODS

A high purity (99.999% purity) sub micrometer (average particle size of 0.2um) alumina powder from Sumitono Chemical Japan (AKP-53) was used to produce a cylindrical pin with a semispherical tip (radius of 2.75mm). The pin was formed by uniaxial followed by isostatic pressing. The sintering was performed in vacuum of 10^{-6} bar for 2 h at 1050°C and 2 h at 1370°C producing 99% of theoretical density pins with an average grain size of 1.2±0.7μm. The disc specimens were made with a 99.5% alumina composition (0.5% of SiO_2). It was prior formed by isostatic pressing and turned into a disc with 75 in diameter and 8 mm of thickness. Subsequently it was sintered at

ISSN 2179-3956

1600°C for 4 h which have led to fully dense microstructure with 2.5±0.5μm average grain size. Finally, the disc surface was finished by machining to a roughness Ra of 0.25± 0.08 μm. The pins ware tested as after sintered, presenting an initial surface roughness Ra of 3.83 ±0.34 μm. The wear tests were conducted in a pin-on-disc machine (Phoenix Tribology -Plint TE-67) at an unlubricated sliding and with load applied by dead weight. The applied loads used were in the range of 2 to 70 N, the sliding speed in the range of 0.1 to 1.0 m/s with constant sliding distance of 5.000m, air humidity of 45±5% and room temperature (20±2°C). Before and after wear test the specimens were ultrasonic cleaned with ethylic alcohol to guarantee a surface free of oil or processing dirties. The wear volume loss was determined from the pin worn scar diameter measured by optical microscopy. Samples with worn surface produced in the mild, transition and severe wear regime were selected for microstructure characterization and roughness. The worn surfaces were studied by scanning electron microscopy (SEM) and optical profilometry.

3 RESULTS AND DISCUSSION

For each speed/load combination tested, Table 1 presents the specific wear rate (W), the W medium scatter (δ) obtained and the wear regime priory characterized from the calculated specific wear rate, assuming that the transition boundary between mild and severe wear regime occurs for W about 10^{-6} mm^3/N.m. Near the transition, the W values may be not sufficient for characterization of the wear regime and some of the results in Table 1 are marked with an interrogation. The sliding speed and applied load combinations were selected in such way to find the mild to transition boundary.

Particularly for points of doubt about the wear regime, marked with the interrogation point at the Table 1, the analysis of the worn surface was made to indentify characteristics such as grooves, ploughing mode, grain pull-out, cracks, intergranular fracture, delamination, as a second criterion for definition of the wear regime. The results of the roughness profile for both pin and disc have been taken as a third criterion. Specific wear rates below 10^{-6} mm^3/N.m and smooth surfaces (Ra above the initial roughness and less than the grain size) are associated with mild regime while grooves, micro-fracture and rate above 10^{-6} mm^3/N.m with severe regime.

To better illustrate the wear behavior changes, from data of Table 1, it was drawn graphs of specific wear rate versus different loads or speed at a constant speed or load, respectively. These graphs are shown at Figure 1 and also from those it could be observed an abrupt behavior change in the specific wear rate (as well the wear severity) at a critical parameter. In the case of the sliding speed, at Figure 1 (a) it could be observed for 40 N the critical sliding speed was 0.3 m/s while for a low load like 10 N the velocity was approximately 0.6 m/s. Now, for the applied loads, as shown in Figure 1 (b), low speeds as 0.2 m/s the load should be in the range of 60 N and 70 N and for 0.4 m/s, about 20 N and 30 N. In addition, the abrupt changes for both graphs, was more expressive and earlier when a higher test severity was imposed (higher load or speed). Besides, those suddenly changes seem to be more significant for the applied load (Figure 1 (b)) than for the sliding speed (Figure 1 (a)). Another interesting fact from observation of Figure 1 and Table 1 is that with the regime change – mild to severe – a higher scatter in the results for the specific wear rates occurred as shown by the error

ISSN 2179-3956

axis. In situations closer to the transition or in the severe regime, the results have presented elevated scatter probably because of brittle fracture of the ceramics. However, the practical interest is on the determination of the specific wear rates in the mild wear since this is the condition in which the material is considered wear resistant.

Table 1: Values of the specific wear rate (W), the W medium scatter (δ) and wear regime with different load/speed combinations. (*Pre-stop represents that test had to be stopped earlier due extensive wear)

Sliding Speed (m/s)	Applied Load (N)	Specific Wear Rate (10^{-6} mm^3/N.m)	δ (10^{-6})	Wear Regime
1.00	10	10.5	3.45	Severe
0.70	2	4.29	4.23	Transition
0.70	5	6.04	1.34	Transition
0.70	10	8.42	4.50	Severe (?)
0.65	2	1.40	1.74	Transition
0.60	5	0.60	0.20	Mild
0.60	10	10.60	3.16	Severe (?)
0.60	20	6.98	3.12	Transition (?)
0.50	10	0.47	0.05	Mild
0.50	20	6.28	0,10	Transition
0.45	30	15.61	3.44	Severe
0.45	40	14.93	2.25	Severe
0.40	10	0.56	0.14	Mild
0.40	20	2.05	0.91	Transition
0.40	30	19.40	7.33	Severe
0.40	40	8.78	3.78	Severe (?)
0.37	30	1.99	0.67	Transition
0.35	30	3.16	1.66	Transition
0.30	20	0.64	0.04	Mild
0.30	40	7.54	6.57	Transition (?)
0.30	50	3.07	1.07	Transition
0.20	30	0.46	0.02	Mild
0.20	40	0.38	0.11	Mild
0.20	50	0.37	0.21	Mild
0.20	60	0.82	0.71	Mild
0.20	70	-	-	Pre-stop*
0.10	60	0.30	0.24	Mild
0.10	70	-	-	Pre-stop*

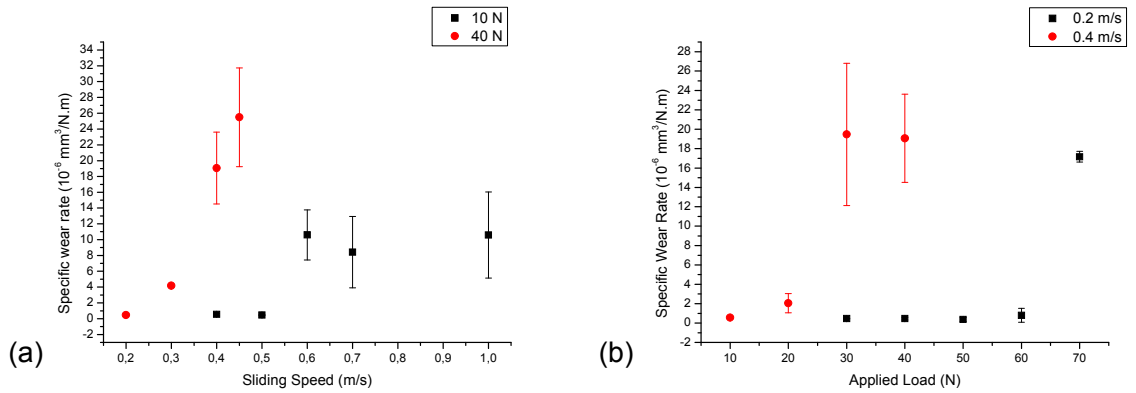

Figure 1. Graphs representing the specific wear rate with the parameters variation: (a) sliding speeds for applied load of 10 and 40 N and (b) applied loads for sliding speeds of 0.2 and 0.4 m/s.

ISSN 2179-3956

Figure 2 shows an example of worn surface characterization. With a load of 20 N at 0.4 m/s, the low magnification image of the wear scar (Figure 2 (a)) shows a well smooth surface (homogeneous), whereas for 0.6 m/s (Fig. 2 (b)) a groove can be clearly observed. For both conditions W values are in the transition regime, however the surface observation has correspondence with the smaller W of test performed at 0.4 m/s. In the case of grooves observation, they were found at both specimens, disc and pin, and the peak and valley roughness coincides well with the matting surfaces since the sliding pair is approximately of the same characteristics. For other applied test loads in the transition or severe regime, the same behavior was found showing that the amount of grooves (and therefore the ploughing micro-abrasion mechanisms) can be associated with higher wear rates. Other observation from low magnification images of the wear scar is that smooth worn surfaces and no significant sign of grooves or fracture are observed when specific wear rates are below $8x10^{-7}$ $mm^3/N.m$. Some authors[1,15,17-19] have associated the wear rate in the range of 10^{-6} to10^{-4} $mm^3/N.m$ with a “transition” condition from mild to severe wear and the worn surfaces analyses of the samples produced in this work allow to observe that this transition occurred in the rage of 10^{-6} $mm^3/N.m$.

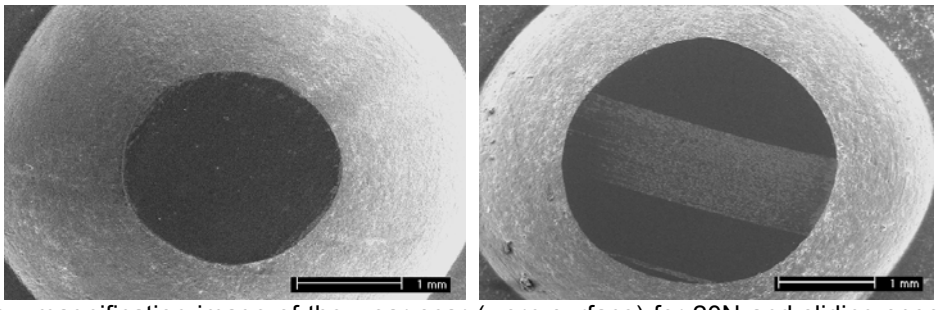

Figure 1. Low magnification image of the wear scar (worn surface) for 20N and sliding speed of: (a) 0.4 m/s and specific wear rate ≈2x10-6 mm3/N.m and (b) 0.6 m/s and ≈7x10-6 mm3/N.m.

In concern about the worn surface it was possible to observe a well defined boundary between severe and mild wear within the speed/load combinations. For example, for samples tested with a 30 N load at 0.2 m/s sliding speed, presenting a specific wear rate of about 10^{-7} $mm^3/N.m$ (mild wear), it was observed a smooth surface as shown at Figure 3 (a), probably due to tribofilm formation. The compacted layer of tribofilm, most likely aluminum hydroxide, was expected due to the relative humidity during the test and is formed by fine particles[6-9]. For a speed of 0.37m/s, Figure 3(b) shows the tribofilm micro-cracking. Although test severity was higher due to higher sliding speed, a little decrease in the wear rate was found. Even being in the error range, this difference might be explained by the unchanged tribofilm’s characteristics. For speeds of 0.4 and 0.45m/s, grooves were present and a tribofilm deformation occurred as shown at Figure 3 (c) and the delayed onset of this region suggest a fatigue phenomenon. For higher sliding speed, since tribofilm detachment was higher (due to delamination), micro-fracture was present and a clearly transition occurred. The groove observed was covered with a layer of very fine wear debris, and the removal of this layer by cleaning uncovers the loss of entire grains by intergranular fracture as shown in Figure 3 (d).

ISSN 2179-3956

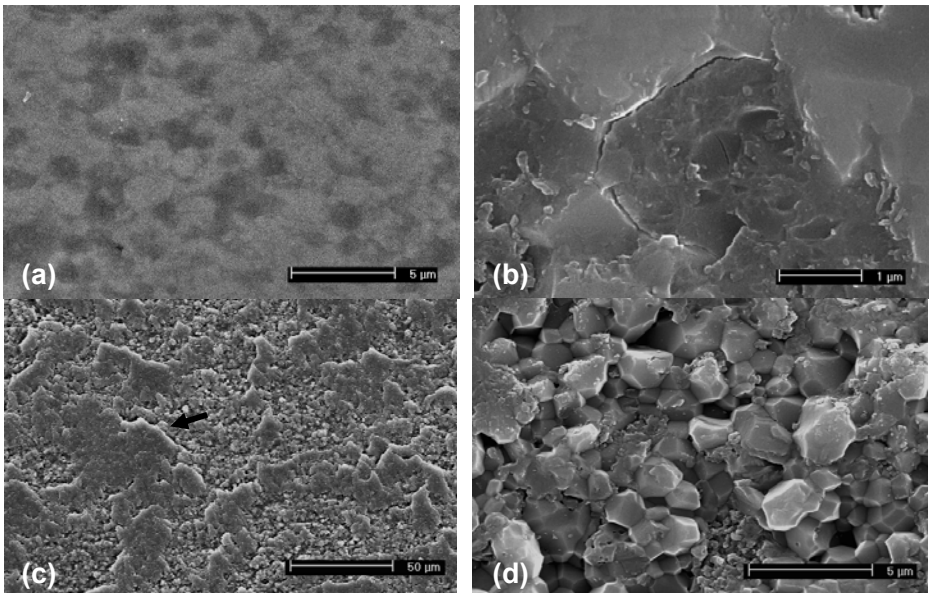

Figure 3: Scanning electron micrographs of the worn surface of the pins after tests with applied load of 30N and different sliding speed: (a) 0.2 m/s, (b) 0.37m/s, (c) 0.40 m/s and (d) 0.45 m/s.

The Figure 4 (a), for 0.2 m/s and 60 N shows a smooth surface but in some extend with grooves (probably due to the micro-ploughing) and plastic deformation of the tribofilm. Increasing the load for 70 N (Figure 4 (b)) it is observed intergranular fracture and grain pull-out as the mean wear mechanism (whereas differently from the fracture presented at Figure 3 (d)). Based on the worn surfaces with higher sliding speed, increasing the speed to 0.4 m/s and decreasing load to 30 N, it was ascertained an extent in the tribofilm plastic deformation and intergranular fracture. The gain in the plastic deformation could be connected to an increase in the local temperature at the point of contact (flash temperature) due to the high speed and the low thermal conductivity coefficient of alumina. In the case of high sliding speed like 0.6 m/s and low load, 10 N, the plastic deformation was the predominantly as shown at Figure 4 (d) and the brittle fracture was observed inside the grooves (Figure 4 (e)). To confirm the earlier hypotheses of wear mechanisms changes and tribofilm formation, in a comparison of the fractures found on the different points of severe wear and different test parameters (Figure 3 (d), Figure 4 (b) and Figure 4 (e)) it was noticed a change from brittle fracture to probably surface fatigue, respectively. From these analyses, it is shown that for conditons of high load and low speeds, it was observed on the worn surfaces situated at the transition or severe regime a slightly plastic deformation with a predominantly intergranular fracture. In contrast, for low loads and high speed, it was found an abundant plastic deformation of the surface.

ISSN 2179-3956

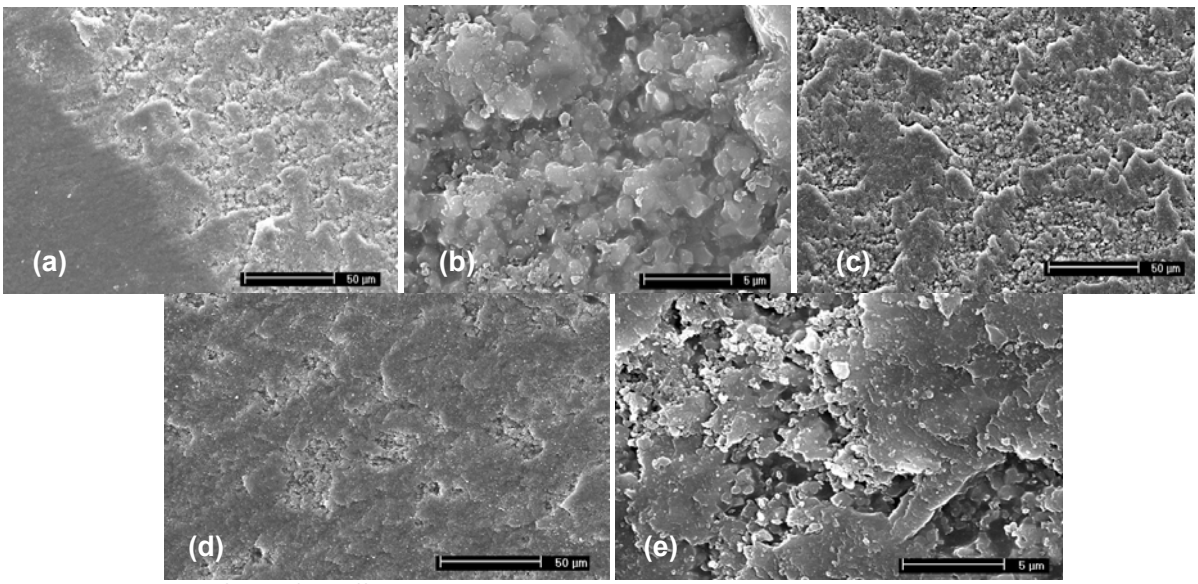

Figure 4.Worn surfaces for different sliding speeds and applied loads representing the transitions in the wear severity: (a) 0.2 m/s and 60 N, (b) 0.2 m/s and 70 N, (c) 0.4 m/s and 30 N, (d) 0.6 m/s and 10 N and (e) fatigue surface inside the plastic deformation.

In concern of the disc roughness, it was observed different patterns with the test parameters. Figure 5 represents the roughness profile of the disc in a (x,y) direction, where x is transversal and y the is longitudinal to the wear track. At low loads (Figure 5 (a) for 0.65 m/s and 2 N) it could be observed a softening of the asperities by the removal of the higher peaks and due to the debris embedded on the wear track, few formation of the tribofilm at the disc and pin occurred (confirmed by worn surface microscopy), whereas little different from those found on other points. Also, the mean roughness Ra for the wear track was higher (Ra ≈ 0.9 µm) than the polished disc (Ra ≈ 0.25 µm). As shown in the literature, the lubricant effect of the tribofilm is confirmed by a smoothing of the initial roughness but it was not found for low loads and high speeds probably because of a change in the wear mechanisms and tribofilm formation due to the applied load and sliding speed. At low load, the quantity of smashed debris is probably smaller due to higher temperature to upward speed compromises the aluminium hydroxide formation but has allowed the plastic deformation of this. By contrast, at average points, like 0.2m/s and 30 N, the roughness profile showed at Figure 5 (b) the occurrence of roughness smoothing on the wear track (in both directions (x,y)) since a well defined tribo-layer was found (showed at Figure 3 (a)). It was confirmed by the Ra values approximately 0.1 µm. The roughness behavior and profile for high loads and minor speeds was inconclusive duo to a high wear of the disc track as can be observed from the profile shown in Figure 5 (c) for 0.1 m/s and 70 N. It is believed, due to the elevated applied load, the pin acted as a harder particle like a diamond stretching a softer material (two-body abrasive wear test) and the mean wear occurred at the disc. As so, the curve had been finished at these points.

ISSN 2179-3956

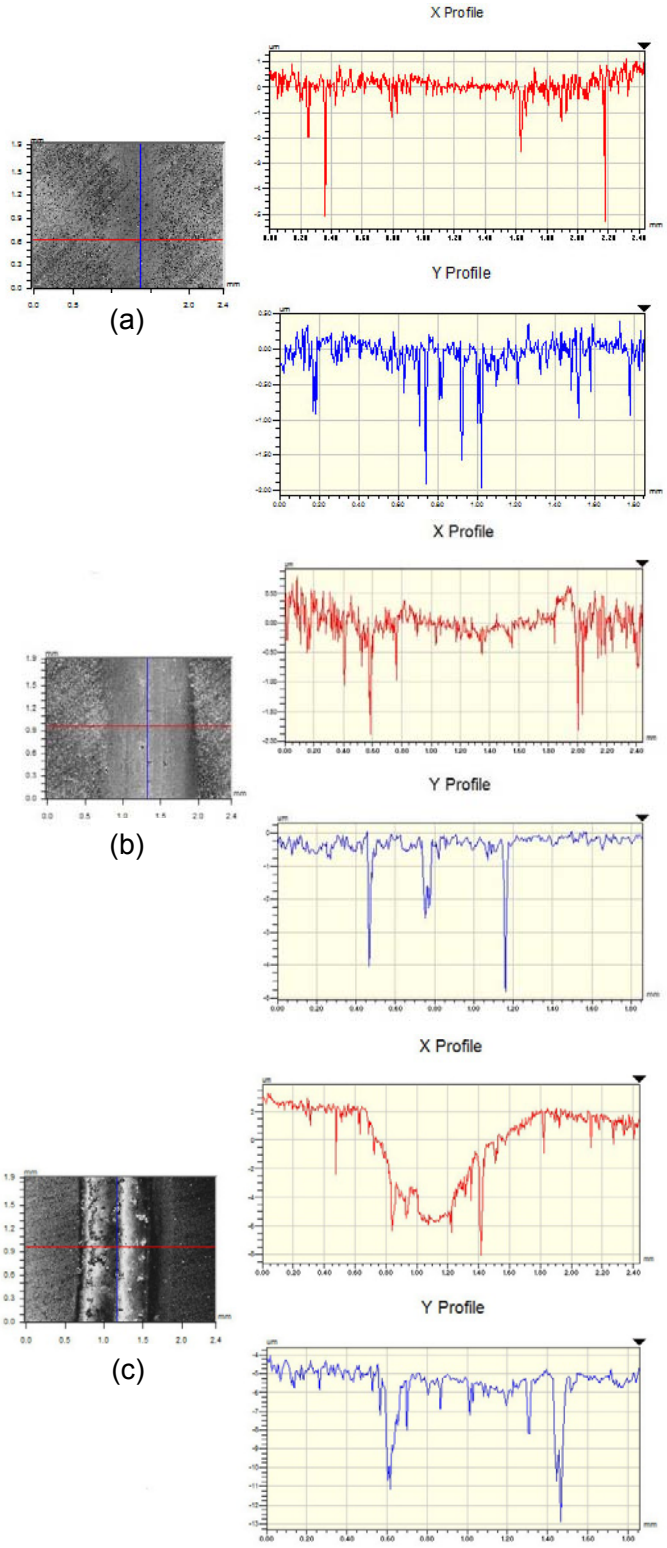

Figure 4. Roughness profile for the disc at different load/speed combinations: (a) 0.65 m/s and 2 N, (b) 0.2 m/s and 30 N and (c) 0.1 m/s and 70 N.

ISSN 2179-3956

Considering data from Table1 and the wear regime characterization, it was possible to drawn a wear diagram for an alumina represented at Figure 6, which shows points of applied load and sliding speed combination representing mild, transition and severe wear regime. In this figure, each point represents the average results of the test. The results near the limit between wear regime were distinguished, not only by the specific wear rate, but also by the image analyses and roughness profiles of the worn surfaces (both pin and disc). The mild wear results are shown as triangular marks, transition as diamonds and severe as quadrangles. It is clearly observed a transition line in between the points representing mild and severe wear. Assuming that below this line the wear will occur in the mild regime, it is possible to define the range of test conditions in which the studied alumina pair (pin and disc) may be present good wear resistance. It is important to be aware that once this diagram for a given material – and so on for other materials – is constructed, it can be used as a material selection guide for engineering applications in similar conditions. Also, the locations of the transition zones likewise the functional dependence provide powerful tools to compare different materials for a given application.

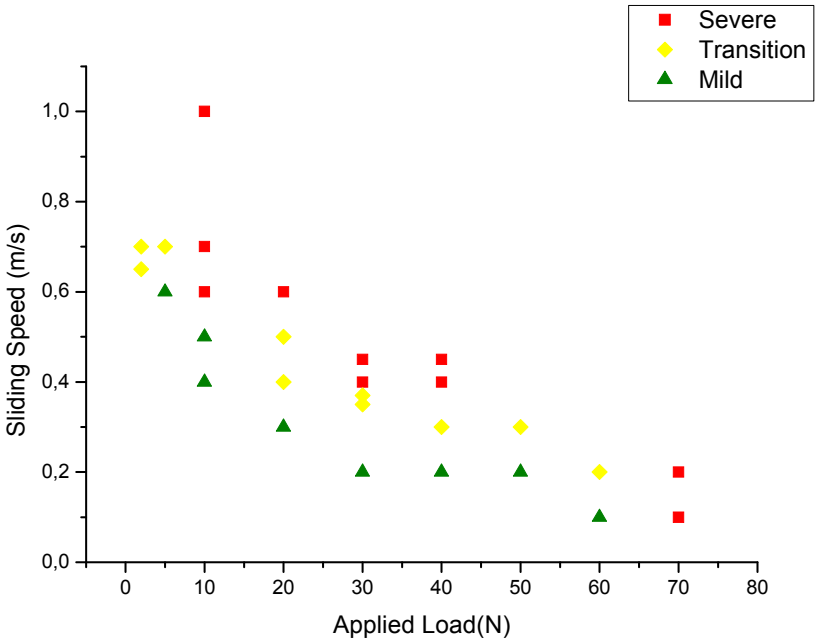

Figure 6. Wear map of applied load versus sliding speed representing the severity wear conditions: mild (triangles), transition (diamonds) and severe (quadrangles).

4 CONCLUSIONS

A pin-on-disc test of high density alumina was performed and the effects of applied load and sliding speed were discussed in terms of the specific wear rate, roughness, worn surface analyzes and the wear severity regime. It was established a boundary curve (simple wear diagram) between mild and severe wear regime with the combination of applied loads and sliding speeds. Also, it was observed the increase of grooves (and therefore the ploughing micro-abrasion mechanisms) with the increase of wear rate. In addition, from the observation of the worn surfaces, the wear regime

ISSN 2179-3956

between the different points combination changes and probably the wear mechanisms due to different behavior on tribofilm formation and delamination.

Acknwledges

The authors would like to acknowledge the governmental institution CNPq, Capes and Fapesp and the UFSCar postgraduate program PPGCEM for the financial support for this research. Also, the authors wish to thank Professor Dr. Renato Goulart Jasinevicius, coordinator of the Laboratório de Usinagem de Precisão from EESC/USP, for the use of the optical profilometry.

REFERENCES

1 HSU, S.; WANG, Y.; MUNRO, R. G.; Quantitative wear maps as a visualization of the wear mechanism transitions in ceramic materials, *Wear*, v. 134, p.1-11, 1989.
2 GEE, M. G.; The formation of aluminium hydroxide in the sliding wear of alumina, *Wear*, v. 153, p.201-227, 1992.
3 AJAYI, O. O.; LUDEMA, K. C.; Mechanism of transfer film formation during repeat pass sliding of ceramic materials, *Wear*, v. 140, p.191-206.
4 ADACHI, K.; KATO, K.; Formation of smooth wear surface on alumina ceramics by embedding and tribo-sintering of fine wear particles, *Wear*, v. 245, p. 84-91, 2000.
5 DENAPE, J.; LAMON, J.; Sliding friction of ceramics: mechanical action of the wear debris, *Journal of Materials Science*, v. 25, p.3592-3604, 1990.
6 YANG, Q.; SENDA, T.; KOTANI, N.; HIROSE, A.; Sliding wear behavior and tribofilm formation of ceramics at high temperatures, *Surface and Coatings Technology*, v. 184, p. 270-277, 2004.
7 ESPOSITO, L.; TUCCI, A.; Microstructural dependence of friction and wear behavior in low purity alumina ceramics, *Wear*, v. 205, p. 88-96, 1997.
8 KATO, K.; ADACHI, K.; Wear of advanced ceramics, *Wear*, v. 253, p.1097-1104, 2002.
9 WANG, Y. S.; HE, C.; HOCKEY, B. J.; LACEY, P. I.; HSU, S. M.; Wear transitions in monolithic alumina and zirconita-alumina composites, *Wear*, v. 181, p. 156-164, 1995.
10 WANG, Y.; HSU, S. M.; The effects of operating parameters and environment on the wear and wear transition of alumina, Wear, v. 195, p. 90-99, 1996.
11 RAVIKIRAN, A.; JAHANMIR, S.; Effect of contact pressure and load on wear of alumina, Wear, v. 251, p. 980-984, 2001.
12 SASAKI, S.; The effect of the surrounding atmosphere on the friction and wear of alumina, zirconia, silicon carbide and silicon nitride, Wear, v. 134, p.185-200, 1989.
13 XIONG, F.; MANORY, R. R.; The effects of test parameters on alumina wear under low contact stress, Wear, v. 236, p.240-245, 1999.
14 BAWJA, S.; RAINFORTH, W. M.; LEE, W. E.; Sliding wear behaviour of SiC-Al2O3 nanocomposites, *Wear*, v.259, p.553-561, 2005.
15 RAINFORTH, W. M.; The wear behaviour of oxide ceramics- A review, *Journal of Materials Science,* v. 39, p.6705-6721, 2004.
16 ANDERSSON, P.; BLOMBERG, A.; Alumina in unlubricated sliding point, line and plane contacts, Wear, v. 170, p.191-198, 1993.
17 ADACHI, K.; KATO, K.; CHEN, N.; Wear map of ceramics, Wear, v.203-204, p.291-301, 1997.
18 HSU, S. M.; SHEN, M. C.; Ceramic wear maps, Wear, v. 200, p.154-175, 1996.
19 CHO, S.-J.; MOON, H.; HOCKEY, B. J.; HSU, S. M.; The transition from mild to severe wear in alumina during sliding, *Acta Mettallurgica Materialia*, v. 40, p.185-192, 1992.